Performance Test of a R134a Centrifugal Water Chiller

Jinhee Jeong*, Pil-Hyun Yoon*, Ghil-Yeung Kim* and Hyeonkoo Lee*

Key words: R134a refrigerant, Centrifugal water chiller, Head coefficient, Flow coefficient

Abstract

A centrifugal water chiller using alternative refrigerant R134a has been developed. The prototype was designed to have refrigerating capacity of 300 RT. Its compressor employs a single high-speed impeller, airfoil diffuser and collector. Newly developed, enhanced tubes were installed in the evaporator and the condenser to reduce the required head for the compressor. Off-design characteristics at various conditions, performance test of the compressor and analysis of the refrigeration cycle were performed. So the probability of use in part load condition was checked and the direction for revision was suggested.

Nomenclature

A : area [m^2]
C : specific heat [kJ/kg · K]
D : impeller diameter [m]
H : polytropic head [m]
h : enthalpy [J/kg]
g : gravity [m/s^2]
$LMTD$: Log mean temperature difference [℃]
$\dot{m}$: mass flowrate [kg/s]
N : rotational speed of impeller [rev/s]
n : polytropic exponent
P : pressure [Pa]
Q : heat [W]
T : temperature [K]
u : impeller tip speed [m/s]
U_{cond} : total heat transfer coefficient of condenser [W/m^2K]
U_{evap} : total heat transfer coefficient of evaporator [W/m^2K]
W : work [W]

Greek symbols

Φ : dimensionless flow coefficient
Ψ : dimensionless head coefficient

Subscripts

e : evaporator
p : polytropic process
r : refrigerant
w : water

* Machinery Research Laboratory, LG Cable Ltd., Kyunggi 431-080, Korea

1. Introduction

Centrifugal chillers and absorption chillers are usually used for industrial or building air-conditioning because of their abilities to handle

large refrigeration capacity. Absorption chillers occupy most of domestic market for commercial air-conditioning system because of governments policy to encourage the use of absorption chiller in order to balance the seasonal phase difference of gas and electricity consumption. However, centrifugal chiller can respond quickly to outside refrigeration load disturbance, has high COP value, and is easy to control. Thus, it occupies most industrial refrigeration market in domestic market and most commercial and industrial market in overseas market. In Korea, centrifugal chillers were first manufactured during late seventies by technical assistance from America and Japan. During early 90's, domestic manufactures succeeded to shift refrigerant from R11 to R123 according to prohibition of use of CFC refrigerants. However, even R123 refrigerant is supposed to fade out in the future due to Montreal protocol. Thus, foreign manufactures finished the development of R134a chiller in the early 90's and most foreign manufactures sell R134a chillers instead of R123 chillers.

Unlike R123 refrigerant, R134a refrigerant has largely different thermodynamic properties, e.g. much higher pressure, and larger density in the refrigeration cycle. Thus, system design needs to be renewed and especially core part of the chiller, i.e. compressor needs to be completely redesigned. We have started to develop a new series of centrifugal chiller using R134a refrigerant from 1996 and succeeded to develop 300 RT model in 1998 as shown in Fig. 1. After that, we kept to improve the efficiency of the refrigerant compressor by redesigning the compressor and testing the performance up to now.

In this paper, we obtained the performance map of the compressor through testing part-load-operation characteristics of the chiller. Through these results, we suggested the next direction of redesign of the compressor and obtained the heat transfer characteristics of condenser tube.

2. Test facility and method

2.1 Test facility

The prototyped centrifugal chiller has an one-stage compressor and the refrigeration cycle consists of four processes as shown in Fig. 2, Table 1 and Fig. 3 show the design specifications of the chiller and the schematic of the compressor respectively. The detailed procedures for compressor design were presented in the paper Lee et al.[1] Test facility consists of a chilled-water pump, a cooling-water pump, a cooling tower, plate-type heat exchangers, a control unit and valves. Since it is difficult to test the prototyped chiller in real building, the

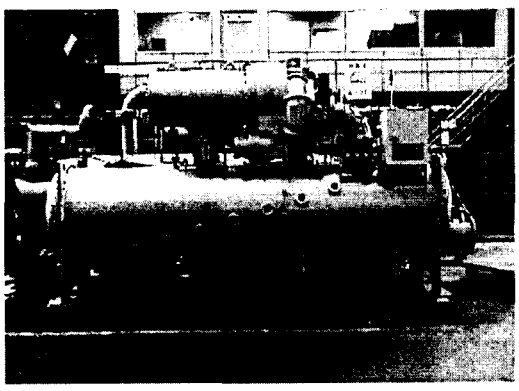

Fig. 1 Developed centrifugal water chiller.

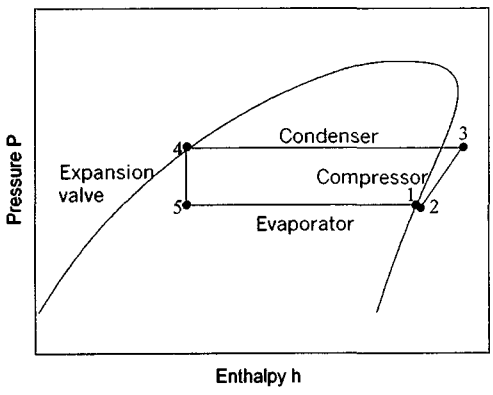

Fig. 2 Refrigeration cycle.

Table 1 Details of the R134a chiller

Compressor	impeller		unshrouded, 11 blades, 11 splitters	
	diffuser		Low Solidity Airfoil type, 9 Airfoils	
	speed		14,400 RPM	
	r_{1h}	33.5 mm	t_{clr}	0.4 mm
	r_{1t}	62 mm	r_5/r_2	1.2281
	r_2	125.2mm	r_6/r_2	1.88698
	r_3/r_2	1.1	D_7	155.2 mm
Heat exchanger	Shell and Tube type			
Expansion device	Fixed orifice and butterfly valve			
Motor	Semi-hermatic, 2 pole, 240 kW			

test facility supplies the chilled water and cooling water according to the Korean Standards (KS). Korean standard (KS) defines the 100% load condition as follows: the inlet and outlet temperature of the chilled water are 12℃ and 7℃ respectively, and the inlet and outlet temperature of the cooling water are 32℃ and 37 ℃ respectively.

Figure 4 (b) shows the points to measure the temperatures and pressures to analyze the chiller's performance. T-type thermocouples are used to measure the temperatures in the refrigerant line. Four-wire-type RTD's are used to measure the temperatures at the inlet and outlet of the chilled and cooling water to reduce the effect of resistance of conducting wire from the sensor to data acquisition system.

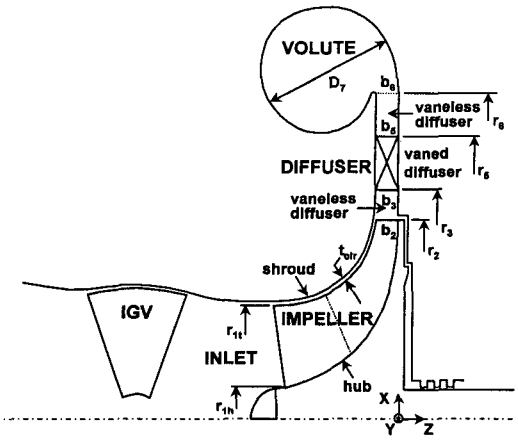

Fig. 3 Schematic of a centrifugal compressor.

Relatively cheap nozzle flowmeters (β=0.75) employing differential pressure transducer (SIEMENS 7MF4432) are used to measure the flowrate of cooling and chilled water because a long straight pipe is available for the measurement. However, it was difficult to install a straight pipe region for the measurement of refrigerant flowrate in the prototyped chiller. Thus, we have installed a cone flowmeter (β= 0.7505) which requires relatively short straight inlet. Except differential pressure, all the pressures are measured by the pressure transducers (Danfoss AKS33 060-G21). To prevent the problem associated with voltage loss from

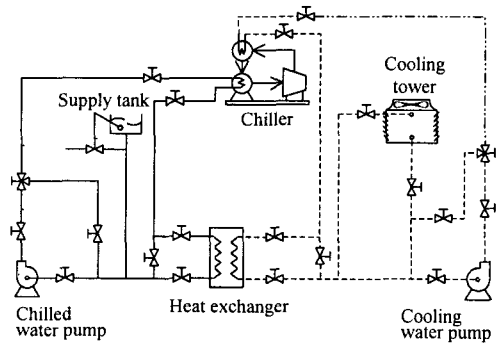

(a) Test rig

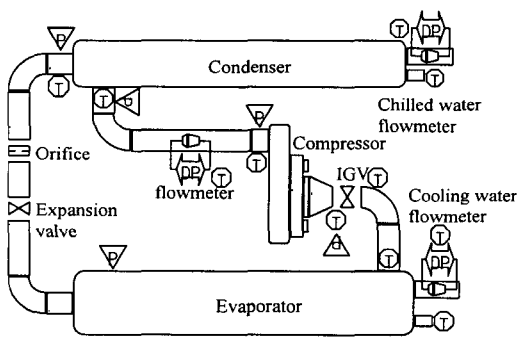

(b) Measuring sensors

Fig. 4 Experimental apparatus for the chiller.

the sensor and acquisition system, all sensors employed the two-wire-type current signals (4~20 mA) instead of voltage signals. These current signals are transformed to the voltage signals before reaching the acquisition system by the precision resistor box, then the analog voltage signals are transformed into digital signals through 16-bit A/D convertor (IOtech DaqBook 2000) and then saved into PC.

2.2 Measurement and data reduction

Since the time scale for temperature fluctuation is large compared to that of pressure fluctuation, we use temperature signal to check the steadiness of the operation. We consider the operation to be steady if the temperature fluctuation maintains to be less than 0.1℃ for 30 minutes, and take measurement data only after signal becomes steady.

To obtain the off-design characteristics of chiller, we first fix the opening of IGV (Inlet Guide Vane) and then change the polytropic head of compressor by controlling condenser inlet water temperature. That is, we increase the condenser inlet water temperature until the compressor experiences the surge phenomenon, and we obtain data at each fixed condenser inlet water temperature. We control the evaporator outlet temperature at 7℃ according to KS standard using controller attached in the chiller, and also measure the inlet and outlet temperature using RTD. KS standard stipulates that evaporator inlet and outlet water temperature is to be 12 and 7℃ respectively and that condenser inlet and outlet water temperature is to be 32 and 37℃ respectively at full load. In part load, evaporator outlet water temperature and condenser inlet water temperature maintain the temperature stipulated at the full load, and the other temperatures change by system itself. The flowrates of evaporator and condenser water are controlled by automatic valves if target temperatures of condenser and evaporator are set. Thus, the flowrates varies significantly depending on temperature conditions.

We need a large amount of tests to complete the part load performance characteristic. In this work, we have two parameters to define the state of compressor, i.e. polytropic head and IGV opening. Thus, we perform a series of tests by increasing polytropic head at fixed IGV opening. From this, we obtain the performance curve of compressor at a fixed IGV opening. The opening rate is set to 0, 20, 40, 60, 80 and 100%. Three to six cases are measured at each opening rate, and in total. A home-made code is used to compute thermodynamic properties of R134a according to the JAR recommendation.[2]

The performance of the compressor varies depending on flowrate, Mach number and Reynolds number, and etc. To ease the analysis, we introduce dimensionless parameters such as flow coefficient and head coefficient as follows.

$$\phi = \frac{q}{ND^3} \tag{1}$$

$$\psi = \frac{gH}{u^2} \tag{2}$$

We can obtain the performance curves of the compressor using these nondimensional parameters computed from the data measured at the partial load condition. If the surge limit and KS operation condition is known, we can obtain the range of part load operation.

The polytropic work can be easily computed as follows if the process within the compressor is supposed to be polytropic.

$$W_p = \int v dp = \frac{n}{n-1} p_2 v_2 \left[\left(\frac{p_3}{p_2} \right)^{(n-1)/n} - 1 \right] \tag{3}$$

where, n is the polytropic exponent and it can be computed from the pressure and temperature at the inlet and outlet of the compressor. Polytropic efficiency is defined to be the ratio of the

polytropic work to actual compressor work as

$$\eta_p = \frac{W_p}{h_3 - h_2} \tag{4}$$

The amount of heat transfer at condenser and evaporator can be expressed in terms of water and refrigerant properties as follows.

$$Q = \dot{m}_w C_w \triangle T_w = \dot{m}_r \triangle h_r \tag{5}$$

In addition, it can be expressed in terms of log mean temperature difference (LMTD) and overall heat transfer coefficient and area as follows.

$$Q = UA \triangle T_{LMTD} \tag{6}$$

The overall heat transfer coefficient U of the heat exchanger depends on geometric characteristics of the heat exchanger, Reynolds number inside tube, temperature difference between refrigerant and water, and bundle effect. For a given chiller, the overall heat transfer coefficient can be expressed in terms of Reynolds number and LMTD as shown in equation (5) and (6).

To indicate the quality of chiller's performance test itself, Air-conditioning and Refrigeration Institute (ARI) defines the percent heat balance as follows

$$\% \text{ heat balance} = \frac{Q_{we} + W_{in} - Q_{wc}}{Q_{wc}} \times 100 \tag{7}$$

and ARI recommends the percent heat balance to be less than 5%.[4]

In Table 2, we can see that the percent heat

Table 2 Reduced experimental data for some load conditions

	Case 1 (20%)	Case 2 (80%)	Case 3 (100%)	Case 4 (100%)	Case 5 (100%)	Case 6 (100%)
Evaporating pressure (kgf/cm^2)	3.94	3.74	3.72	3.73	3.74	3.91
Evaporating temperature (℃)	7.87	6.33	6.17	6.28	6.37	7.63
Pressure, compressor inlet (kgf/cm^2)	3.57	3.59	3.57	3.59	3.62	3.81
Temperature, compressor inlet (℃)	6.82	5.91	5.75	5.88	6.00	7.34
Pressure, compressor outlet (kgf/cm^2)	9.30	10.08	10.14	10.22	10.36	10.79
Temperature, compressor outlet (℃)	40.20	40.40	40.22	40.07	50.00	50.55
Mass flow rate (kg/s)	5.251	7.153	7.712	7.596	7.202	6.386
Shaft work (kW)	153.4	206.1	219.7	218.3	212.5	198.2
Flow coefficient	0.0740	0.1062	0.1151	0.1129	0.1067	0.0908
Head coefficient	0.515	0.589	0.595	0.598	0.605	0.606
Polytropic efficiency (%)	62.9	72.9	74.4	74.1	73.0	69.6
Condensing pressure (kgf/cm^2)	9.25	9.99	10.03	10.12	10.27	10.73
Condensing temperature (℃)	35.81	38.62	38.76	39.09	39.67	41.30
Entering condenser water temperature (℃)	31.15	31.97	31.54	32.01	33.01	35.69
Leaving condenser water temperature (℃)	34.59	36.71	36.64	37.02	37.76	39.67
Volume flow rate, cooling water (m^3/h)	215.96	221.7	223.83	223.27	221.5	219.06
Heat flux, cooling water (kW)	864.6	1220.8	1326.1	1301.4	1223.3	1013.6
Entering chilled water temperature (℃)	11.46	11.46	11.78	11.79	11.50	11.68
Leaving chilled water temperature (℃)	8.49	6.93	6.91	7.02	7.06	8.09
Volume flow rate, chilled water (m^3/h)	191.65	186.97	190.46	189.83	189.79	190.36
Heat flux, chilled water (kW)	663.21	984.42	1077	1051.9	979.17	794.44
Cooling capacity (RT)	188.7	280.1	306.45	299.29	278.6	226.04
Consumption power (kW)	164	220	231	232	225	210
kW/RT	0.869	0.785	0.754	0.775	0.808	0.929
Q_w ($Q_{wc} - Q_{we}$)	201.39	236.38	249.1	249.5	244.13	219.16
Heat balance (water, %)	4.32	1.34	1.36	1.34	1.56	0.90
Heat balance (refrigerant, %)	0.60	0.63	0.86	0.71	0.79	0.81

balance satisfies the limit specified by ARI. In the ARI standard, Q_e and Q_c are supposed to be calculated from data for the cooling and chilled water temperature. In addition to the method specified by ARI to compute Q_e and Q_c, we also consider computing it from the refrigerant-side data i.e. (1) enthalpy difference of refrigerant at inlet and outlet and (2) mass flowrate of the refrigerant. The heat balances computed using water-side data and refrigerant-side data are 4.96% and 1.16% respectively.

3. Results and discussions

3.1 Performance analysis of the heat exchanger

We show, in Fig. 5, the overall heat transfer coefficients of the condenser at the various conditions which is unintentionally accompanied from the test condition of compressor. It is found that the experimental data is well approximated by an equation.

$$U_{cond} = \frac{4764.5}{\sqrt{LMTD}} + 2736.1 \qquad (8)$$

Since the correlation is very good, it can be concluded that the overall heat transfer coefficient depends almost only on LMTD and decreases with increasing LMTD as expected from the single tube experiment. In the all LMTD range, the overall heat transfer coefficient exceeds 5000 W/m^2K, so that the value is comparable to that of evaporator tube.

In the test, we have used designed condenser tubes (similar to Wolverine's Turbo-C type which is quite popular in the industry). The overall heat transfer coefficient for a single tube is already published as the experimental result.[5] However, the result for single tube is much higher than the current result, which is expected from the bundle effect. In designing condenser in the future, we plan to use the equation (8) instead of the single tube result.

3.2 Performance analysis of the chiller

Figure 6 shows the variation of LMTD's of condenser and evaporator as the refrigeration load changes. The LMTD's of both condenser and evaporator increase with increasing refrigeration load as it is expected. In Fig. 6, the ratio of RT to LMTD is defined to be the overall heat transfer coefficient. The ratio of RT to LMTD keeps constant in evaporator with increasing RT, because the slope is straight. However, the ratio of condenser decreases with increasing refrigeration load as it is consistent with the result from the Fig. 5.

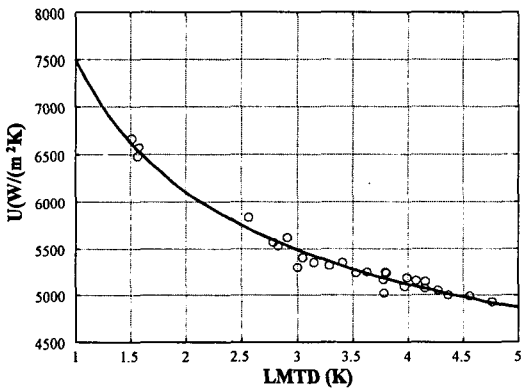

Fig. 5 Overall heat transfer coefficient of the condenser.

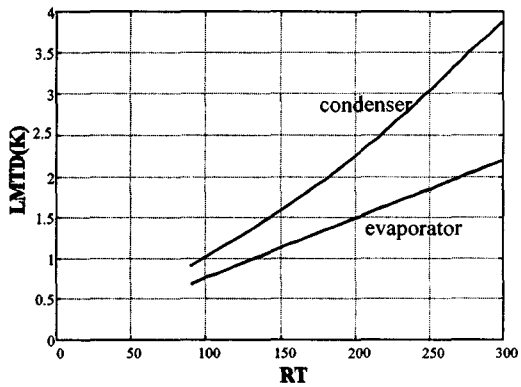

Fig. 6 Variation of LMTD for heat exchangers with respect to cooling load.

The Compressor is definitely the most important sub-assembly among the parts of the centrifugal chiller. Its performance is directly related to the operation range of the chiller and its efficiency is the most influential factor for the chiller efficiency. To indicate the efficiency of the chiller, we usually use the power consumption to unit refrigeration ton denoted as kW/RT. Thus, the smaller value means the better efficiency. Figure 7 shows the variation of the chiller efficiency to the refrigeration load. Here load 1.0 indicates the full load. As in the figure, the efficiency of the prototype chiller at the full load is found to be 0.76 kW/RT. This means that the efficiency level of R134a improves by 10~15% from the one of old-fashioned R123 centrifugal chiller and approaches to the one of product of the leading foreign manufacturers. Until the refrigeration load decreases from 100% to 80%, the chiller efficiency improves a little up to 0.75 kW/RT. However, as the refrigeration load decreases below 80%, the chiller efficiency deteriorates steeply shown in Fig. 8, although the polytropic head keeps decreasing. The reason for this is because the compressor efficiency decreases drastically below 80% refrigeration load. To look at this more carefully, we draw the variation of the compressor efficiency alone to refrigeration load. At the full load, the compressor

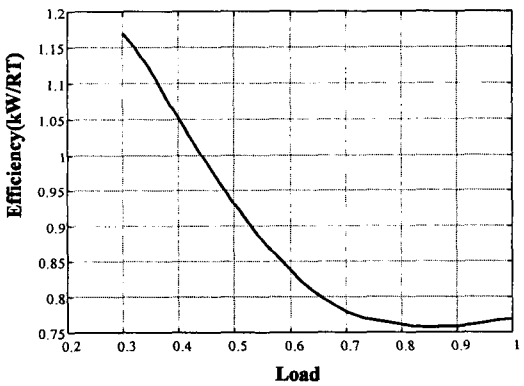

Fig. 7 Chiller efficiency for part load conditions.

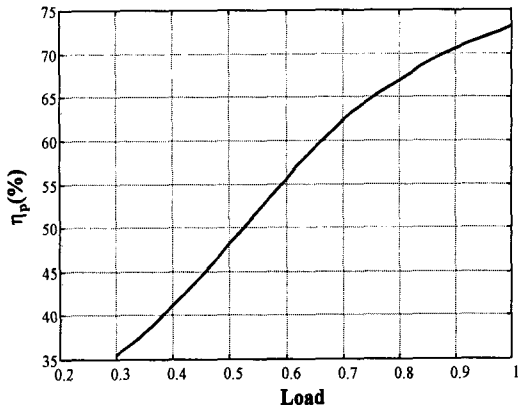

Fig. 8 Polytropic efficiency of compressor for part load conditions.

efficiency is only 74%, which is 6% less than our target at the design stage. As the refrigeration load decreases, the compressor efficiency keeps decreasing. The reason why the chiller efficiency increases a little bit is because the polytropic head decreases faster than the compressor efficiency decreases as the refrigeration load decreases from 100% to 80%. Since the compressor efficiency of the full load condition is only 74%, there are still some margin to improve, and we expect that we can catch up the chiller efficiency (around 0.68 kW/RT) of the leading companies at the full load condition if the compressor efficiency improves above 80%.

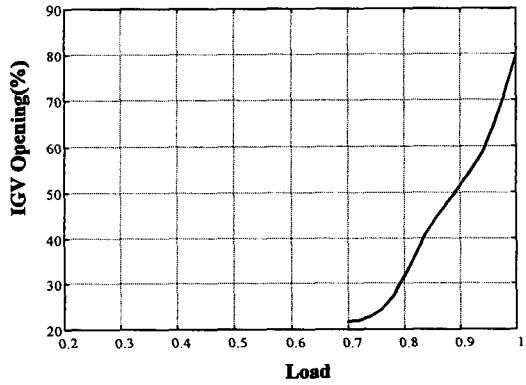

Fig. 9 IGV opening for part load conditions.

Figure 9 shows IGV opening rate to the refrigeration load. It shows that IGV opening is almost less than 20% at refrigeration loads below 70%. This implies that the IGV does not play a role for controlling the refrigeration load below 70%. In the test, we have experienced the surge several times when the refrigeration load was less than 70%. Since the industry requires that the operation range of the centrifugal chiller be 30~100%, our prototyped chiller definitely has problems associated with the operational range. This problem has to be solved before commercialization stage and we will discuss the solution to this problem later in the paper.

Figure 10 shows the variation of the refrigeration capacity per unit mass flowrate of refrigerant as the refrigeration load changes. As the refrigeration load decreases, the refrigeration capacity per unit mass flowrate increases. This can be explained in terms of refrigeration cycle. As the refrigeration load decreases, the condenser pressure decreases according to the KS condition. Thus, point 4 in Fig. 2 moves to the bottom left, so that the quality at the point just before the evaporator decreases. Since the refrigeration capacity per unit mass is the same as the length of line 5-1 in Fig. 2, the decreased quality increases the refrigeration capacity per unit mass.

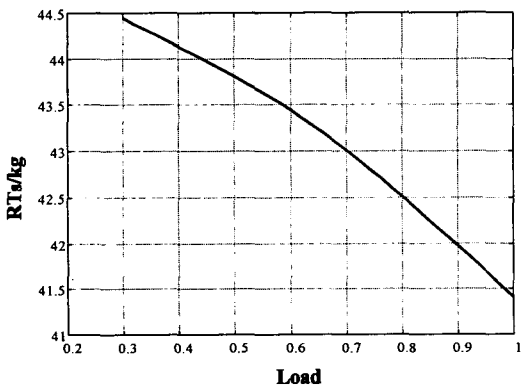

Fig. 10 Refrigeration load per mass flow rate for part load conditions.

In Fig. 11, we show the performance map for the prototyped compressor for different IGV opening rate. The coordinates are given in terms of flow and head coefficients.

The operation line of the chiller for the KS condition is shown as the solid line with lower slope and the surge line is indicated by the steeper solid line. The surge line was obtained from joining surge points which was determined from the experiments at fixed IGV opening. The surge line was obtained through the linear curve fitting with surge points. In turn, the surge point distinguishes itself as the severe fluctuation of severe fluctuation of the static pressure in condenser and evaporator.

The curved lines denoted as ① to ⑥ in Fig. 11 are the iso-efficiency curves of the compressor and shows that the compressor efficiency increases as IGV opening increases as expected. Since the line corresponding to KS condition needs to be located below the surge line for surge-free operation, the operational range in the flow coefficient is just 0.82~0.11. Thus, the range of part load which can be handled is too small, and thus we need some modifications.

A simplest modification can be easily suggested from the nondimensional argument, i.e., to increase the impeller's diameter by 7.7% (D' =0.2696) while keeping the impeller's shape

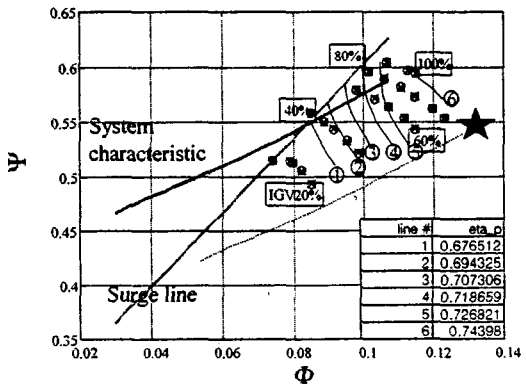

Fig. 11 Performance map of the compressor.

the same. Thereby, we can shift the full load point in Fig. 11 to the location marked with a asterisk. In this case, the dimensionless performance curve would not change even if the diameter increases; in addition to that, the line of KS condition can be shifted to the dotted line starting at the point marked "asterisk". Thus, the operation range in terms of flow coefficient can be as large as 0.04~0.132, which means that the operation range can be 30~100% of full load. In the case, the flow and head coefficients are 0.132 and 0.54 respectively. The refrigeration capacity grows large to be 390 RT; of course, we can secure a large surge margin as well.

4. Conclusions

The part-load performance of the prototyped centrifugal chiller which was originally designed for the full load condition only is tested in real condition, and we obtained the following results.

(1) The chiller efficiency is confirmed to be 0.76 kW/RT which is close to the original target (0.75 kW/RT).

(2) The operation range is severely limited by the surge line and operation below the load of 70% refrigeration load was difficult.

(3) We have suggested the design modification to secure the surge margin and to obtain the proper operation range.

(4) We also obtained the condenser's overall heat transfer coefficient which is above 5000 W/m^2K for all LMTD ranges.

Acknowledgments

This research is a part of the project of the cleaner production technology, "Development of R134a centrifugal chiller". It was supported by Korea Institute of Industrial Technology and Ministry of Commerce, Industry and Energy. Thanks to the persons concerned. We also inform that the project for this paper was finished three years ago, so that the current status of chiller design is far ahead of the level mentioned in the paper.

References

1. Lee, Y., Jeong, J., Kim, J. and Lee, C., 2000, Design of the Centrifugal Compressor for a R134a Turbo-Chiller, Proceedings of the SAREK 2000 Summer Annual Conference (II), pp. 435-442.
2. Japanese Association of Refrigeration and Japan Flon Gas Association, 1991, Thermophysical Properties of Environmentally Acceptible Fluorocarbons (HFC-134a and HCFC-123), Japanese Association of Refrigeration.
3. ASHRAE, 1996, Heating, Ventilating, and Air-Conditioning Systems and Equipment, Handbook 34-1996.
4. Air-conditioning and refrigeration institute, 1998, Standard for water chilling packages using the vapor compression cycle (Standard 550/590), p. 21.
5. LG Cable Ltd., 1999, Development of high performance heat exchanger (Turbo-B type evaporator/condenser), Ministry of Commerce, Industry and Energy.